

Robust trajectory tracking control for unmanned surface vessels under motion constraints and environmental disturbances

Proc IMechE Part M:
J Engineering for the Maritime Environment
1–18

© IMechE 2021



Article reuse guidelines:

sagepub.com/journals-permissions

DOI: 10.1177/14750902211039663

journals.sagepub.com/home/pim



Ruo Zhang, Yuanchang Liu  and Enrico Anderlini 

Abstract

To achieve a fully autonomous navigation for unmanned surface vessels (USVs), a robust control capability is essential. The control of USVs in complex maritime environments is rather challenging as numerous system uncertainties and environmental influences affect the control performance. This paper therefore investigates the trajectory tracking control problem for USVs with motion constraints and environmental disturbances. Two different controllers are proposed to achieve the task. The first approach is mainly based on the backstepping technique augmented by a virtual system to compensate for the disturbance and an auxiliary system to bound the input in the saturation limit. The second control scheme is mainly based on the normalisation technique, with which the bound of the input can be limited in the constraints by tuning the control parameters. The stability of the two control schemes is demonstrated by the Lyapunov theory. Finally, simulations are conducted to verify the effectiveness of the proposed controllers. The introduced solutions enable USVs to follow complex trajectories in an adverse environment with varying ocean currents.

Keywords

unmanned surface vehicle, input constraints, maritime environments, backstepping control, trajectory tracking

Date received: 23 October 2020; accepted: 26 July 2021

Introduction

The term unmanned surface vessels (USVs) refers to marine vehicles that can achieve the required operation on the water surface autonomously.¹ USVs can be widely used for various applications in the maritime sector, including transportation, environmental investigation, resources exploration and military operations.² Since USVs do not require any human intervention, the deployment of USVs can potentially increase personal safety, operational range and precision and flexibility in a harsh environment.³ Therefore, the research and development of USVs have become a significant part of marine robotics with substantial effort contributed by many researchers and engineers in recent decades.⁴ In particular, the increasing reliance on the ocean has stimulated a growing demand for the development of USVs.

To ensure safe navigation of USVs, an autonomous navigation system (ANS) is the most critical part. In general, an ANS consists of three essential capabilities, including sensing/perception, planning and control. Among them, the control module directly operates on autopilot and propels USVs to robustly follow the

defined trajectories. Consequently, the design of a robust controller for USVs is of pivotal importance and is associated with challenges such as systems nonlinearity and uncertainties, underactuation of vessels dynamics, control input saturation, external disturbances, etc.⁵ These problems leave challenges to the researchers and demonstrate the need for further development for USVs.

In essence, the development of control strategies is oriented by different control objectives, including: (1) set point control, (2) path following control and (3) trajectory tracking control.³ Setpoint control forces the position and heading of the ship to the desired value without time requirement. It is the most basic control objective and plays an important role in dynamic

Department of Mechanical Engineering, University College London, London, UK

Corresponding author:

Yuanchang Liu, Department of Mechanical Engineering, University College London, Roberts Engineering Building, London WC1E 7JE, UK.

Email: yuanchang.liu@ucl.ac.uk

position for fixed target operation such as autonomous docking.⁶ However, setpoint control cannot be achieved using continuous control inputs.³ Therefore, it is only used in some special missions and does not attract much interest from researchers.

Path following control requires a USV to follow a specified path with a certain speed without temporal constraint.⁷ It can be achieved by using a continuous controller and has less stringent control requirements than trajectory control. The most popular approach to achieve the path following control is by using the Lookahead-based line-of-sight (LOS) guidance law.⁵ The basic idea is to mimic the performance of a helmsman, setting the course angle based on the ratio of the cross-track error and look ahead distance.⁸ Based on the LOS guidance law, Zheng and Sun⁹ proposed using a backstepping technique augmented by radial basis function neural network (RBFNN) and an auxiliary design system to achieve the path following control. A finite-time currents observer based ILOS guidance law combined with the adaptive technique are used in Fan et al.⁷ to address the path following control.

Different from the path following control, of which the path has no temporal constraint, trajectory tracking control requires a USV to track a trajectory with spatial and temporal constraints.¹⁰ Therefore, it is more general and compatible to handle more complicated missions. Thus, as the complexity of the missions has increased, further development for trajectory control is required. The trajectory tracking control of USVs can be mainly divided into control of the fully actuated ship and control of the underactuated ship,³ with the former being already reasonably understood, whereas the understanding of the latter still limited.

More specifically, USVs with common configurations have only two controls, that is the surge force and yaw moment, while the sway axis is not actuated. Thus, the motion of three degrees of freedom will be controlled by only two inputs, which makes it a typical underactuation problem.⁹ Several control methods have been attempted to realise the trajectory tracking for underactuated USV, including the backstepping technique,¹¹ sliding mode control,¹² model predictive control,¹³ dynamic surface control,¹⁴ linear algebra-based approach,¹⁵ and intelligent control strategies.¹⁶ The most popular methods are the backstepping technique, which is usually combined with Lyapunov's direct method, and sliding mode control that characterises the tracking error through the use of the sliding surface. As the sliding mode can suffer from chattering effects and imposes high loads on the actuator, the backstepping technique is used more in the trajectory tracking problem.⁵ The basic idea behind the backstepping technique is to treat some of the states as 'virtual controls', and then design the virtual control laws as the control through Lyapunov's direct method.⁹ Pettersen and Egeland¹⁷ firstly proved that a USV system was controllable and raised a potential control law. However, only exponential stability was obtained. Dong et al.¹⁸

used a controller based on modified backstepping technique and enriched by integral action and achieved the trajectory tracking control with better steady and transient performance.

The above-mentioned control scheme for trajectory tracking control does not take the motion constraints into consideration. Therefore, the desired actuator's output and the vehicle's velocity can be infinite, so that input saturation is required. The ignorance of the input saturation will lead to performance degradation, lag, overshoot, as well as instability in the closed-loop response of practical systems.⁹ For this reason, it is of great theoretical and practical significance to design a control scheme to handle motion constraints. The motion constraints mainly include the constraints of the yaw torque and surge velocity. A Gaussian error function has been used to approximate the input saturation of the actuators and globally uniform ultimate boundedness of the system was achieved. Wang and Zhang¹⁹ designed an auxiliary design system to handle input saturation through adaptive control. However, these studies mostly focus on the saturation limit of the actuator, while the constraints of the velocity are always ignored. Therefore, these controllers must be developed by taking the velocity constraints into consideration.

Apart from the input saturation, another vital factor that is ignored in many studies is the external disturbance caused by the ocean current. Without the consideration of the environmental disturbance, a ship will deviate from the desired trajectory. Chen²⁰ proposed that, for a general control system with disturbance, the disturbance can be cancelled by setting the control input to be linearly dependent on the disturbance. However, this method cannot be directly used for realising the trajectory tracking of USVs due to their underactuated nature. Fossen and Lekkas²¹ used the sign function inside the controller to handle the disturbance. However, this method may make the system chatter and introduced discontinuous control variables. Zhu and Du²² used an adaptive estimate law and a finite-time disturbance observer to handle the external disturbances. Qiu et al.²³ proposed a sliding mode surface control scheme cooperated with adaptive technology to deal with the external disturbance. These control methods mainly used adaptive estimation law, mostly cooperated with disturbance observer, to estimate and compensate for the unknown ocean currents, which suits for situations that the ocean currents are hard to be measured.

The ocean current velocity can be measured in real time with acoustic doppler profilers installed on the bottom of the vessel integrated with global positioning systems.^{24,25} Thus, it is possible to design a control scheme based on known ocean current information. In the current literature of trajectory tracking control for unmanned systems, some controllers are designed based on the kinematic model only,^{26,27} and some also incorporate the full dynamic model.^{19,22} The advantage of the controller based on the kinematic model is that it can be easily applied in commercial unmanned vehicles

cooperated with a well-developed propulsion system, which only requires the velocity signals to control the ship.²⁸ In addition, control algorithms based on the kinematic model can be easily extended into the control of multiple USVs,²⁹ as most current research on coordination control is based on the kinematic model due to the complexity of the system.³⁰ As the focus of this study is on the constraints and influence of external disturbances on the velocity, considering only the kinematic model is more suitable for this problem, while the control of the dynamic systems can be easily achieved independently through the backstepping technique. Thus, it is possible to design a control scheme based on known ocean current information. Motivated by the above reasons, this paper develops two robust control schemes to achieve the trajectory tracking control for the USV under motion constraints with and without considering external disturbances. The effectiveness of both control schemes is verified through numerical simulations. The contribution of the study can be summarised as follow:

1. The external disturbance is considered in this study and a virtual system is introduced to handle it. It is proved that using the virtual system, the model of the USV can be simplified and the derived velocity can compensate for the ocean current.
2. Based on the virtual system, the backstepping technology combined with the Lyapunov direct method are used to calculate the desired control law. It is proved that the control scheme demonstrates excellent performance to achieve the trajectory tracking control of the USV with normal ability to handle the input saturation in complicated environments.
3. In order to improve the ability to handle the input saturation, a controller based on the normalisation technique is used to normalise the tracking error and thereby to make the velocity be related to the design parameters and reference trajectories, which can produce smoother input compliant with the practical limitation.
4. By using the virtual system, the complicated environmental disturbance can be solved by a simple method that has excellent performance.

The rest of the paper is organised as follow. Section 2 introduces the problem formulation, including the model of the USV and the transformation to the virtual. Section 3 presents the design of the control law. Section 4 presents the simulation results of the proposed approaches and the discussion of the result. Then the conclusion of this study and the future work are presented in section 5.

Problem formulation

The motion of a marine surface vessel is shown in Figure 1. It is described based on two different orthogonal coordinates: the inertial and body-fixed reference frames. The inertial coordinate is fixed to the earth,

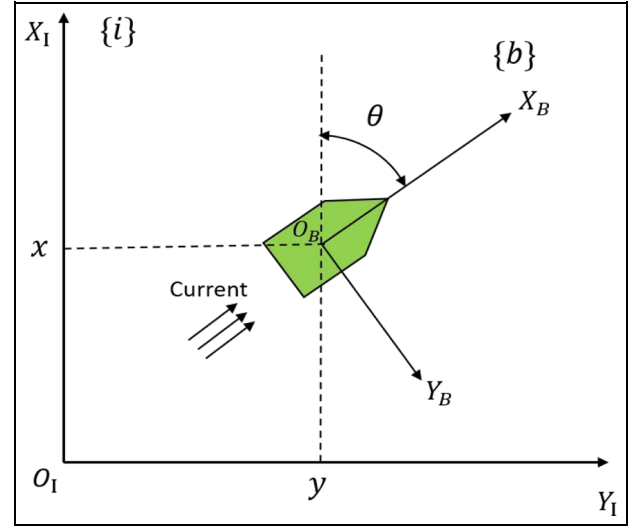


Figure 1. Motion of a USV.

with the origin located at a fixed point, the x -axis pointing to the north and the y -axis pointing to the east. The body-fixed reference frame is fixed to the ship. The USV is assumed to be symmetrical with zero trim, and the origin of the attached body-fixed frame is set to match the centre of gravity, which is satisfied for most commercial surface vessels.^{23,31} The x -axis points to the heading of the ship and the y -axis is perpendicular to the x -axis. The USV model in the presence of disturbance can be written as⁷

$$\begin{cases} \dot{x} = u_r \cos \theta - v_r \sin \theta + V_x \\ \dot{y} = u_r \sin \theta + v_r \cos \theta + V_y \\ \dot{\theta} = \omega \end{cases} \quad (1)$$

where u_r and v_r are the relative surge and sway velocities; x , y and θ are the position of the USV in the inertial frame. V_x and V_y are the environmental disturbances.

The velocity in the sway axis is small and can readily converge to zero through the control of the dynamics. Hence, it can be neglected when calculating the desired linear velocity and yaw rate.

Thus, the motion of the USV can be simplified as follows

$$\begin{bmatrix} \dot{x} \\ \dot{y} \\ \dot{\theta} \end{bmatrix} = \begin{bmatrix} \cos \theta & 0 \\ \sin \theta & 0 \\ 0 & 1 \end{bmatrix} \begin{bmatrix} v \\ \omega \end{bmatrix} + \begin{bmatrix} V_x \\ V_y \\ 0 \end{bmatrix} \quad (2)$$

Assumption 1. The environmental disturbances considered in this study are irrotational, time-varying and bounded.

Due to the practical limitation, the velocity cannot exceed the capacity of the engine. Therefore, there exist limits for the input velocity, which can be expressed as

$$\begin{cases} |v| \leq v_{max} \\ |\omega| \leq \omega_{max} \end{cases} \quad (3)$$

where v_{max} and ω_{max} are positive constants representing the saturation bounds from practical restriction.

In the model of the USV, if the disturbance can be cancelled out, the derivatives of the states will become the function of only the states and inputs. Then the complexity of the system will be reduced, and the problem can be solved by using the same method as the model without the disturbance. Based on this observation and inspired by the idea of cancelling the disturbance through setting the input as a function of disturbance, virtual inputs and heading angle are introduced, which satisfy the following condition

$$\begin{cases} v_t \cos \theta_t = v \cos \theta + V_x \\ v_t \sin \theta_t = v \sin \theta + V_y \\ \dot{\theta}_t = \omega_t \end{cases} \quad (4)$$

where v_t and θ_t physically represent the absolute velocity and the heading angle of the USV under the influence of ocean currents. After the implementation of the virtual system, the motion system is simplified and transformed into a virtual system

$$\begin{bmatrix} \dot{x} \\ \dot{y} \\ \dot{\theta}_t \end{bmatrix} = \begin{bmatrix} \cos \theta_t & 0 \\ \sin \theta_t & 0 \\ 0 & 1 \end{bmatrix} \begin{bmatrix} v_t \\ \omega_t \end{bmatrix} \quad (5)$$

The reference to be tracked is assumed to be

$$\begin{bmatrix} \dot{x}_r \\ \dot{y}_r \\ \dot{\theta}_r \end{bmatrix} = \begin{bmatrix} \cos \theta_r & 0 \\ \sin \theta_r & 0 \\ 0 & 1 \end{bmatrix} \begin{bmatrix} v_r \\ \omega_r \end{bmatrix} \quad (6)$$

Assumption II. The reference linear and angular velocities are bounded and smaller than the limitation of the USV velocity.

$$\begin{cases} \sup_{t \geq 0} |v_r(t)| \leq v_{max} \\ \sup_{t \geq 0} |\omega_r(t)| \leq \omega_{max} \end{cases} \quad (7)$$

Remark II. This assumption is practical, as the reference velocity cannot exceed the capacity of the engine. Otherwise, the ship can never achieve the tracking assignment.

Then the tracking error, which is the difference between the trajectory and the USV in the body-fixed frame, can be expressed as

$$\begin{bmatrix} x_e \\ y_e \\ \theta_e \end{bmatrix} = \begin{bmatrix} \cos \theta_t & \sin \theta_t & 0 \\ -\sin \theta_t & \cos \theta_t & 0 \\ 0 & 0 & 1 \end{bmatrix} \begin{bmatrix} x_r - x \\ y_r - y \\ \theta_r - \theta_t \end{bmatrix} \quad (8)$$

where x_e and y_e are the along-track error and the cross-track error, which represent the difference along the x-axis and y-axis in the body-fixed frame and θ_e is the radial-track error, representing the difference of the heading angle.

According to (5), (6) and (8), the error dynamics, which are the derivatives of the tracking error of the system, can be expressed as

$$\begin{bmatrix} \dot{x}_e \\ \dot{y}_e \\ \dot{\theta}_e \end{bmatrix} = \begin{bmatrix} \omega y_e + v_r \cos \theta_e - v_t \\ -\omega_t x_e + v_r \sin \theta_e \\ \omega_r - \omega_t \end{bmatrix} \quad (9)$$

The control objective now is to find the suitable control input $u_t = (v_t, \omega_t)^T$ to stabilise the system in (9), which requires that $\lim_{t \rightarrow \infty} (|x(t) + y(t) + \theta(t)|) = 0$.

The dynamic model is not considered in the design of the controller, but it could be used to verify the effectiveness of the proposed controller in the future. The dynamic model of the USV is⁷

$$\begin{cases} \dot{u}_r = \frac{m_{22}}{m_{11}} v_r \omega - \frac{d_{11}}{m_{11}} u_r - \sum_{i=2}^3 \frac{d_{ui}}{m_{11}} |u_r|^{i-1} u_r + \frac{1}{m_{11}} \tau_u \\ \dot{v}_r = -\frac{m_{11}}{m_{22}} u_r \omega - \frac{d_{22}}{m_{22}} v_r - \sum_{i=2}^3 \frac{d_{vi}}{m_{11}} |v_r|^{i-1} v_r \\ \dot{\omega} = \frac{m_{11} - m_{22}}{m_{33}} u_r v_r - \frac{d_{33}}{m_{33}} \omega - \sum_{i=2}^3 \frac{d_{ri}}{m_{11}} |r|^{i-1} r + \frac{1}{m_{33}} \tau_1 \end{cases} \quad (10)$$

where $u_r = v$ is the surge velocity; m_{ij} ($j = 1, 2, 3$) are the inertia including added mass; d_{ii} , d_{ui} , d_{vi} and d_{ri} are the linear and quadratic hydrodynamic damping in the surge, sway and yaw.

The proposed controller will output the desired surge velocity and yaw rate, which could be used to calculate the relative sway velocity based on equation (10). Then required torque to force the sway, surge velocity and the yaw rate to the desired value could be readily obtained through backstepping technology.

Control law design

In this section, two different trajectory tracking control schemes for USVs will be proposed. For the first controller, based on the virtual system, the backstepping technique and Lyapunov's direct method will be used to calculate the required control law, which will finally be limited by the auxiliary system to handle the input saturation. The second controller will use the normalisation technique to make the inputs relate to the reference trajectory and design parameters only. Then, the

input will be limited to the saturation limit by tuning of the design parameters.

Control law based on the backstepping technique

The first control scheme is mainly designed based on the backstepping technique and Lyapunov's direct method. At first, to solve the undersaturation problem, the backstepping technique is used, which treats two tracking errors as virtual control inputs to stabilise the other states and design the intermediate control laws that depend on the dynamics state. Then, based on that, Lyapunov's direct method is used to find the desired control law that stabilises the tracking error to 0.

A common USV only has control in the surge and yaw degrees of freedom, while sway is not actuated. Therefore, y_e cannot be directly controlled. According to the backstepping technique, θ_e and x_e are chosen as the virtual control inputs to stabilise y_e . To find the immediate control laws, the candidate Lyapunov function is chosen as $V_y = \frac{1}{2}y_e^2$. Then, in the view of (9), the derivative of V_y is

$$\dot{V}_y = y_e \dot{y}_e = -\omega_t y_e x_e + v_r \sin \theta_e y_e \quad (11)$$

The virtual control is assumed as $\theta_e = 0$, and $x_e = k_1 \varphi(y_e)$, where k_1 is a positive design parameter. Then \dot{V}_y becomes $-k_1 \omega_t y_e \varphi(y_e)$. To stabilise the system, $\varphi(x_e)$ must be uniformly continuous and makes \dot{V}_y negative definite. Thus, $\varphi(y_e)$ must satisfy the following condition:

1. In the domain of the system, φ has derivatives of all orders (C^∞).
2. $\varphi(0) = 0$.
3. $z\varphi(z) > 0$.
4. φ is bounded.

Examples of $\varphi(y_e)$ is $\omega_t y_e$, $\sin(\arctan \omega_t) y_e$, and $\frac{1-e^{2k\omega_t}}{1+e^{2k\omega_t}} y_e$. The range of $\sin(\arctan \omega_t) y_e$ is $[-1, 1]$. As the velocity will be directly related to the control laws by using this method, $\sin(\arctan \omega) y_e$ can avoid producing extremely large design control laws. Thus, it is chosen as the intermediate control law, the error between x_e and intermediate control law is set as

$$\bar{x}_e = x_e - k_1 \sin(\arctan \omega_t) y_e \quad (12)$$

Then the x_e is transformed into

$$\begin{aligned} \dot{\bar{x}}_e &= \dot{x}_e - k_1 \cos(\arctan \omega_t) \frac{1}{1+\omega_t^2} \dot{\omega}_t y_e \\ &\quad + k_1 \sin(\arctan \omega_t) (-\omega_t x_e + v_r \sin \theta_e) \\ &= -v_t + \omega_t y_e + v_r \cos \theta_e - k_1 \cos(\arctan \omega_t) \\ &\quad \left(\frac{1}{1+\omega_t^2} \right) \dot{\omega}_t y_e - k_1 \sin(\arctan \omega_t) \omega_t x_e \\ &\quad + k_1 v_r \sin(\arctan \omega_t) \sin \theta_e \end{aligned} \quad (13)$$

A new variable α is introduced to simplify the above equation, which is defined as

$$\begin{aligned} \alpha &= v_r \cos \theta_e + k_1 \left(-\cos(\arctan \omega_t) \frac{\dot{\omega}_t}{1+\omega_t^2} y_e \right. \\ &\quad \left. - \sin(\arctan \omega_t) \omega_t x_e + v_r \sin(\arctan \omega_t) \sin \theta_e \right) \end{aligned} \quad (14)$$

Then $\dot{\bar{x}}_e$ is simplified to

$$\dot{\bar{x}}_e = -v + \omega_t y_e + \alpha(v, v_r, \omega, \dot{\omega}, x_e, y_e, \theta_e). \quad (15)$$

After the intermediate control law is defined, the next step is to find the desired control law through Lyapunov's direct method. Consider the candidate Lyapunov function

$$V = \frac{1}{2} \bar{x}_e^2 + \frac{1}{2} y_e^2 + \frac{2}{k_3} \left(1 - \cos \frac{\theta_e}{2} \right) \quad (16)$$

Then, the derivative of the V yields

$$\begin{aligned} \dot{V} &= \bar{x}_e \dot{\bar{x}}_e + y_e \dot{y}_e + \frac{1}{k_3} \sin \frac{\theta_e}{2} \dot{\theta}_e \\ &= \bar{x}_e (-v_t + \alpha) + \frac{1}{k_3} \sin \frac{\theta_e}{2} (-\omega_t + \omega_r + 2k_3 v_r \cos \frac{\theta_e}{2} y_e) \\ &\quad - k_2 \omega_t \sin(\arctan \omega_t) y_e^2 \end{aligned} \quad (17)$$

According to the property of the function that $z\varphi(z) \geq 0$, it can be verified that $-\omega_t \sin(\arctan \omega_t) y_e^2 \leq 0$. To guarantee that \dot{V} is negative definite, the choice of ω_t and v_t must make the rest term negative definite. Based on this idea, the following control law is chosen

$$\begin{cases} v_t = \alpha + k_2 \bar{x}_e \\ \omega_t = \omega_r + 2k_3 v_r \cos \frac{\theta_e}{2} y_e + k_4 \sin \frac{\theta_e}{2} \end{cases} \quad (18)$$

where k_2 , k_3 and k_4 are positive design parameters.

The stability of the system with the proposed controller can be proved as follow.

Proposition 1. If $v_r(t)$ and $w_r(t)$ are uniformly continuous at $[0, +\infty)$ and do not converge to 0 at the same time, then by using the control law (18), the system (9) is globally asymptotically stable.

Proof At first, for the convenience of expression, the Barablat lemma is introduced.

Lemma 1. (Barbalat lemma)

If $x(t)$ is differentiable and bounded at $[0, +\infty)$, and $\dot{x}(t)$ are uniformly continuous, then it can be concluded that $\lim_{t \rightarrow \infty} \dot{x}(t) = 0$.

The Lyapunov scalar function contains all the control states that can reflect the stability of the control and is positive definite.

Substituting (18) into (16) yields,

$$\dot{V} = -k_1 \bar{x}_e^2 - k_2 \omega_t \sin(\arctan \omega_t) y_e^2 - \frac{k_4}{k_3} \sin^2\left(\frac{\theta_e}{2}\right) \quad (19)$$

As k_1, k_2, k_3 and k_4 are positive constants and $\sin(\arctan \omega_t) \geq 0$, $\dot{V} \leq 0$, which implies that V is non-decreasing with time and $V(t) \leq V(0)$. Since V is positive definite and uniformly bounded, x_e, y_e and θ_e are uniformly bounded. Then according to the error dynamics (9), \dot{x}_e, \dot{y}_e and $\dot{\theta}_e$ are also uniformly bounded, which in turn demonstrates that x_e, y_e and θ_e are uniformly continuous. Then, since the control laws are functions of $x_e, y_e, \theta_e, \dot{x}_e, \dot{y}_e, \dot{\theta}_e, v_r$ and ω_r , which are all uniformly continuous, it can be proved that v_t and ω_t are uniformly continuous. Thus, all the term in \dot{V} are uniformly continuous, which further proves that \dot{V} is uniformly continuous.

V is differentiable and bounded and \dot{V} is negative definite. Thus, according to the Barbalat Lemma, $\lim_{t \rightarrow \infty} \dot{V} = 0$. In view of (19), $\lim_{t \rightarrow \infty} \bar{x}_e^2 = 0$, $\lim_{t \rightarrow \infty} \omega_t \sin(\arctan \omega_t) y_e^2 = 0$ and $\lim_{t \rightarrow \infty} \sin^2\left(\frac{\theta_e}{2}\right) = 0$. According to the assumption that when $t \rightarrow \infty$, v_r and ω_r do not converge to 0 at the same time, ω_t never converges to 0, implying that $\omega_t \sin(\arctan \omega_t) \neq 0$. Thus, $\lim_{t \rightarrow \infty} y_e^2 = 0$ and thereby $\lim_{t \rightarrow \infty} y_e = 0$, which in turn implies that $k_1 \sin(\arctan \omega_t) y_e$ converges to 0. As it can also be proved that $\lim_{t \rightarrow \infty} x = k_1 \sin(\arctan \omega_t) y_e$ from $\lim_{t \rightarrow \infty} \bar{x}_e = 0$, then it can be concluded that x converges to 0. As $\lim_{t \rightarrow \infty} \sin\left(\frac{\theta_e}{2}\right) = 0$, it can be concluded that θ_e converges to 0. Thus, it can be proved that, by using the control law (18), $\lim_{t \rightarrow \infty} (|x(t) + y(t) + \theta(t)|) = 0$, which means the system (9) is uniformly asymptotically stable.

After deriving the virtual control law, the next step is to obtain the actual control input.

According to (4), the real control input satisfies the following condition,

$$\begin{aligned} v \cos \theta &= v_t \cos \theta_t - V_x \\ v \sin \theta &= v_t \sin \theta_t - V_y \end{aligned} \quad (20)$$

Then by rearranging (20)

$$\begin{cases} v = \sqrt{v_t^2 + V_x^2 + V_y^2 - 2v_t(V_x \cos \theta_t + V_y \sin \theta_t)} \\ \theta = \text{artan2}(v_t \sin \theta_t - V_y, v_t \cos \theta_t - V_x) \\ \omega = \frac{\dot{v}_t(V_y \cos \theta_t - V_x \sin \theta_t) + v_t \omega_t(v_t - V_x \cos \theta_t - V_y \sin \theta_t) + v(\dot{V}_x \sin \theta - \dot{V}_y \cos \theta)}{v^2} \end{cases} \quad (21)$$

The above system may induce velocity beyond the limitation. The following auxiliary system is used to handle input saturation. Taking the input saturation of the linear and angular velocity into consideration, the final input generated by the ships are $sat(v)$ and $sat(\omega)$. The saturation function is

$$sat(x) = \begin{cases} x_{max}, & \text{if } |x| > x_{max} \\ x, & \text{if } -x_{max} \leq x \leq x_{max} \\ -x_{max}, & \text{if } x < -|x_{max}| \end{cases} \quad (22)$$

where x representing v and ω , x_{max} and x_{min} is the upper and lower limit of the velocity.

The full control block for the control scheme based on the backstepping technique augmented by the virtual system and auxiliary system are shown in Figure 2.

The designed controller can stabilise the error, and the performance, such as the response time and the smoothness of the control input, can be adjusted by changing the control parameters. The problem of the above designed controller is that the resulting linear and angular velocity may change sharply when it reaches the upper and lower bounds. Thus, the next method based on normalisation is proposed. The maximum and minimum velocity derived in the next controller can be set in a fixed range by changing the control parameter. Therefore, by setting the maximum and minimum velocity within the physical limitations, the sharp change of the inputs will not occur, thus resulting in better performance of the system. However, due to the uniqueness of the design, the second method is not able to handle the external disturbance. In the next section, the detail of the second method will be introduced.

Control law based on the normalisation technique

The basic idea of the normalisation technique is to normalise certain tracking errors appropriately to make the designed velocity bounded by design parameters and the reference velocity only. The controller does not take the disturbance into consideration, as the virtual system used in the last method cannot be normalised. Thus, the model of the USV without disturbance is used in this method, which is

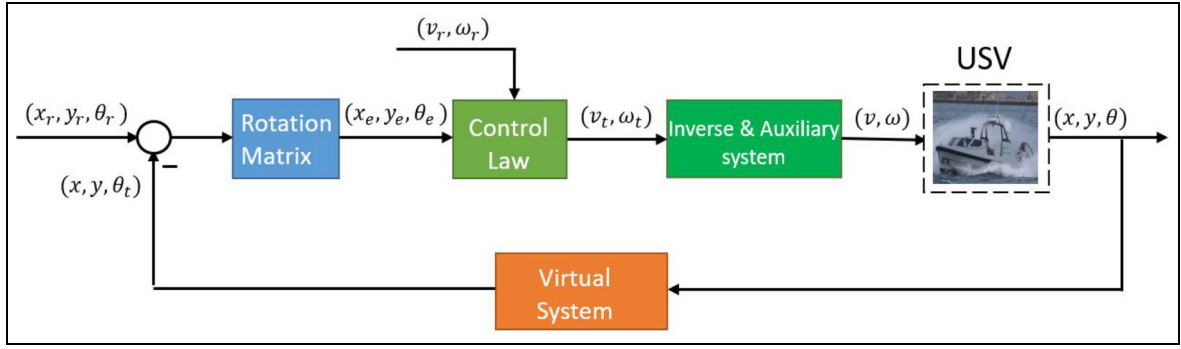


Figure 2. Block diagram for the closed-loop system based on the backstepping technique.

$$\begin{bmatrix} \dot{x} \\ \dot{y} \\ \dot{\theta} \end{bmatrix} = \begin{bmatrix} \cos \theta & 0 \\ \sin \theta & 0 \\ 0 & 1 \end{bmatrix} \begin{bmatrix} v \\ \omega \end{bmatrix} \quad (23) \quad \begin{cases} v_1 = v_r \cos \theta_e + \varphi(x_e) \\ \omega_1 = \omega_r + \frac{1}{k_1} v_r y_e + g(\theta_e) \end{cases} \quad (29)$$

The error dynamics based on the above system are

$$\begin{bmatrix} \dot{x}_e \\ \dot{y}_e \\ \dot{\theta}_e \end{bmatrix} = \begin{bmatrix} \omega y_e + v_r \cos \theta_e - v \\ -\omega x_e + v_r \sin \theta_e \\ \omega_r - \omega \end{bmatrix} \quad (24)$$

To further simplify the error dynamics, the new control input is defined, which is

$$\begin{bmatrix} u_0 \\ u_1 \end{bmatrix} = \begin{bmatrix} \omega_r - \omega \\ v_r \cos \theta_e - v \end{bmatrix} \quad (25)$$

Then error dynamics are changed to

$$\begin{bmatrix} \dot{x}_e \\ \dot{y}_e \\ \dot{\theta}_e \end{bmatrix} = \begin{bmatrix} (\omega_r - u_0)y_e + u_1 \\ -(\omega_r - u_0)x_e + v_r \sin \theta_e \\ u_0 \end{bmatrix} \quad (26)$$

To find the errors that need to be normalised, let us first consider a candidate Lyapunov function like the one used in the first method, which is

$$V_1 = \frac{1}{2}x_e^2 + \frac{1}{2}y_e^2 + k_1(1 - \cos \theta_e) \quad (27)$$

where k_1 is positive design parameters.

Taking the time derivative of the scalar function along (26) yields

$$\begin{aligned} \dot{V}_1 &= x_e[(\omega_r - u_0)y_e + u_1] \\ &\quad + y_e[-(\omega_r - u_0)x_e + v_r \sin \theta_e] + k_1 u_0 \sin \theta_e \\ &= x_e u_1 + k_1 \sin \theta_e \left(u_0 + \frac{1}{k_1} v_r y_e \right) \end{aligned} \quad (28)$$

To make \dot{V} negative, the control as designed as follow

where $\varphi(x_e)$ is a function satisfying $x_e \varphi(x_e) \geq 0$ and $g(\theta_e)$ is function satisfying $\sin \theta_e g(\theta_e) \geq 0$.

As $|v_r \cos \theta_e| \leq |v_r|$, the linear velocity in (29) can be bounded inside the specified range by choosing a suitable $\varphi(x_e)$ that satisfies $\varphi(x_e) \leq v_{max} - \sup_{t \geq 0} |v_r|$. Conversely, due to the term $v_r y_e$, the angular velocity is directly related to the cross-track error. Thus, it cannot be bounded inside the limitation if the tracking error is large. To address that problem, y_e needs to be normalised. The common way is to normalise the range of y_e to unity by using $\frac{y_e}{\sqrt{1+y_e^2}}$. However, as y_e and x_e are not independent, y_e is normalised as $\frac{y_e}{\sqrt{1+x_e^2+y_e^2}}$. Then, the candidate Lyapunov function is changed accordingly to

$$V = \sqrt{1 + x_e^2 + y_e^2} + k_1(1 - \cos \theta_e) \quad (30)$$

Taking the derivative of (30) along (26) yields,

$$\begin{aligned} \dot{V} &= \frac{x_e \dot{x}_e + y_e \dot{y}_e}{\sqrt{x_e^2 + y_e^2 + 1}} + k_1 u_0 \sin \theta_e \\ &= \frac{x_e u_1}{\sqrt{x_e^2 + y_e^2 + 1}} + k_1 \sin \theta_e \left(u_0 + \frac{v_r \sin \theta_e y_e}{k_1 \sqrt{x_e^2 + y_e^2 + 1}} \right) \end{aligned} \quad (31)$$

To make the derivative of the Lyapunov function negative definite, the following function was chosen

$$\begin{cases} u_0 = -\frac{v_r y_e + k_2 g(\theta_e)}{k_1 \sqrt{x_e^2 + y_e^2 + 1}} \\ u_1 = k_3 \varphi(x_e) \end{cases} \quad (32)$$

where k_2 and k_3 are control parameters, $g(\theta_e)$ is a function satisfying $\sin(\theta_e)g(\theta_e) \geq 0$ and $\varphi(x_e)$ is a function satisfying $x_e \varphi(x_e) \leq 0$. To bound the input, $g(\theta_e)$ and $\varphi(x_e)$ are chosen as $\sin \theta_e$ and $\frac{2}{\pi} \arctan(k_4 x_e)$, which satisfies the above requirement and ranges from -1 to 1 .

Thus, the designed control law is

$$\begin{cases} \omega = \omega_r + \frac{v_r y_e + k_2 \sin \theta_e}{k_1 \sqrt{x_e^2 + y_e^2 + 1}} \\ v = v_r \cos \theta_e + \frac{2}{\pi} k_3 \arctan(k_4 x_e) \end{cases} \quad (33)$$

Take two new parameters β, γ satisfying the following condition

$$\begin{aligned} 0 < \beta &\leq \omega_{max} - \sup_{t \geq 0} |\omega_r(t)| \\ 0 < \gamma &\leq v_{max} - \sup_{t \geq 0} |v_r(t)| \end{aligned} \quad (34)$$

For the control for ω and v

$$\begin{cases} |\omega| \leq |\omega_r| + \left| \frac{v_r y_e + k_2 \sin \theta_e}{k_1 \sqrt{x_e^2 + y_e^2 + 1}} \right| \leq \sup_{t \geq 0} |\omega_r(t)| + \frac{|v_r|_{max} + k_2}{k_1} \\ |v| \leq |v_r \cos \theta_e| + \left| \frac{2}{\pi} k_3 \arctan(k_4 x_e) \right| \leq |v_r| + k_3 \leq \sup_{t \geq 0} |v_r| + k_3 \end{cases} \quad (35)$$

By adjusting the parameters k_1, k_2 and k_3 to satisfy the following condition,

$$\begin{aligned} \frac{\sup_{t \geq 0} |v_r(t)| + k_2}{k_1} &\leq \beta \\ k_3 &\leq \gamma \end{aligned} \quad (36)$$

the linear and angular velocity will become

$$\begin{cases} |\omega| \leq \sup_{t \geq 0} |\omega_r(t)| + \beta \leq \omega_{max} \\ |v| \leq \sup_{t \geq 0} |v_r| + \gamma \leq v_{max} \end{cases} \quad (37)$$

Thus, the linear and angular velocity will never go beyond the limit of the engine.

The stability of the system will be proved as follow.

Proposition 2. If $v_r(t), \omega_r(t)$ are uniformly continuous at $[0, +\infty)$, then by using the control law (33) with design parameters satisfying condition (35), the system (26) is globally asymptotically stable and the reference trajectory is asymptotically tracked.

Proof. Substituting (35) into (31) yields

$$\dot{V} = - \frac{\frac{2}{\pi} k_3 x_e \arctan(k_4 x_e) + k_2 \sin^2 \theta_e}{\sqrt{1 + x_e^2 + y_e^2}} \leq 0 \quad (38)$$

$\dot{V} \leq 0$ illustrates that V decrease with time and thereby $V(t) \leq V(0)$, which means that V is uniformly bounded. Since V is positive definite and uniformly bounded, x_e, y_e and θ_e are also bounded.

Then, taking the second order derivatives of the Lyapunov function yields

$$\begin{aligned} \ddot{V} = & - \frac{\frac{2k_3 k_4 \dot{x}_e}{\pi(1+k_4^2 x_e^2)} + k_2 \dot{\theta}_e \sin(2\theta_e)}{1+x_e^2+y_e^2} \\ & + \frac{(x_e \dot{x}_e + y_e \dot{y}_e) \left(\frac{2}{\pi} k_3 x_e \arctan(k_4 x_e) + k_2 \sin^2 \theta_e \right)}{(1+x_e^2+y_e^2)^{\frac{3}{2}}} \end{aligned} \quad (39)$$

It is already proved that $x_e, y_e, \theta_e, v, \omega, v_r, \omega_r$ are bounded. Then, from the error dynamics (24), it can be proved that \dot{x}_e, \dot{y}_e and $\dot{\theta}_e$ are bounded. Since all the terms in \ddot{V} are bounded, \ddot{V} is also bounded. Hence, \dot{V} is uniformly continuous. By Barbalat's lemma, it can now be proved that $\lim_{t \rightarrow \infty} \dot{V} = 0$. Thus, $\lim_{t \rightarrow \infty} x_e \arctan(k_4 x_e) = 0$ and $\lim_{t \rightarrow \infty} \sin^2 \theta_e \rightarrow 0$, which in turn implies that $\lim_{t \rightarrow \infty} x_e = 0$ and $\lim_{t \rightarrow \infty} \theta_e = 0$. The next step is to prove $\lim_{t \rightarrow \infty} y_e = 0$.

Substituting the control law of ω in (33) into the error dynamics of θ_e in (24) yields

$$\dot{\theta}_e = \frac{v_r y_e + k_2 \sin \theta_e}{k_1 \sqrt{x_e^2 + y_e^2 + 1}} \quad (40)$$

Since it has been proved that θ_e is bounded and $\dot{\theta}_e$ is uniformly continuous, it can be proved that $\lim_{t \rightarrow \infty} \dot{\theta}_e \rightarrow 0$ by Barbalat's lemma. Since $\lim_{t \rightarrow \infty} x_e = 0, \lim_{t \rightarrow \infty} \theta_e = 0$ and $\lim_{t \rightarrow \infty} \dot{\theta}_e = 0$, according to (40), it can be concluded that $\lim_{t \rightarrow \infty} y_e = 0$. According to the above proof, the global asymptotic stability of the system has been proved. The control block diagram of this controller is shown in Figure 3.

Comparison between the proposed control method and model predictive control (MPC)

The method proposed in this paper and the MPC method are both based on the known USV model. However, compared with the MPC method, the proposed controller algorithm has a smaller computational cost and is thus more applicable to a real-time implementation. At each sample time, the MPC method needs to calculate the future states and solve the optimisation problem along the prediction horizon, which requires a powerful and large processor.³² For the proposed control algorithms, only the current states need to be calculated at each time step, which saves significant computational cost and space.

In addition, conventional MPC requires the existence of a state feedback controller. However, according to Brockett's condition, a state feedback controller cannot stabilise the underactuated system.³³ Thus, conventional nonlinear model predictive control (NMPC) is not applicable for USVs. To apply NMPC to the control of USVs, many other stringent constraints and

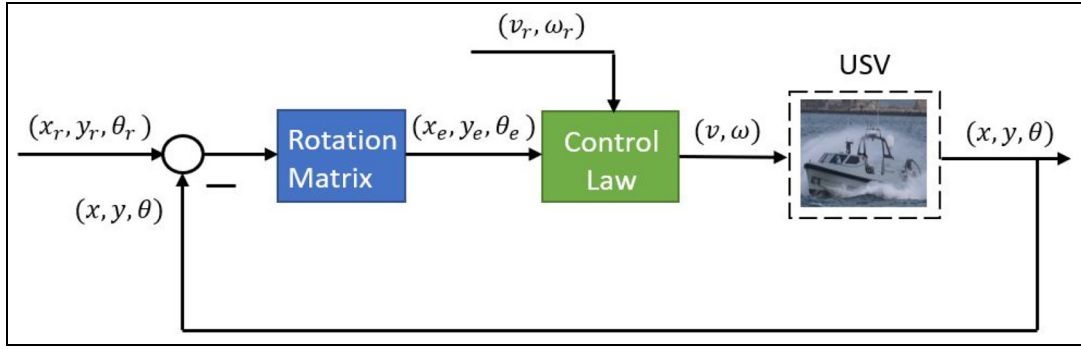


Figure 3. Block diagram for the control system based on normalisation technique.

Table 1. Control parameters of USV simulations.

Scenario	Controller 1 (BS)				Controller 2 (NL)			
	k_1	k_2	k_3	k_4	k_1	k_2	k_3	k_4
1	0.15	0.15	0.001		40	2		
2	0.2	0.2	0.004		50	8		
3	0.1	0.1	0.001		100	10		
4	0.01	0.1	0.05		30	3		

condition need to be applied, which adds to the complexity of the control scheme and increases the computation cost.^{34,35} Besides, some conditions such as forecasting the evolution of the disturbances, etc. are challenging and cannot be achieved in the practical world, which limits the application range of the MPC method. Thus, compared with the MPC method, the proposed controller is more suitable for the real-time trajectory tracking control of USVs.

Simulations

In order to verify the effectiveness of the proposed control schemes for the trajectory tracking control of the USV, simulations are conducted in the MATLAB environment. All simulations were performed on Intel i7 2.60 GHz octa-core CPU with 16 GB RAM. The controllers are tested in four different scenarios: (1) circular trajectory with constant ocean currents, (2) sinusoidal trajectory with constant ocean currents, (3) sinusoidal trajectory with time-varying ocean currents and (4) minimum snap trajectory with time-varying currents. In the fourth scenario, a real case is studied, where the USV is required to pass five stations on the sea to deliver cargos under time-varying ocean currents and berthed at the last stations. The trajectory passing the five stations are generated by the minimum snap method, which produces a smooth and optimal trajectory with a minimum snap under certain dynamic constraints.^{18,36} Performance comparisons between the two proposed controllers and the PID controllers^{37,38} are presented in the first scenarios. Then in the rest of the scenarios, only the proposed controllers are tested. Besides, the controller based on the normalisation

technique is tested without considering the ocean currents. The result for the controller based on backstepping technology is marked as BS and the controller based on normalisation technique is marked as NL.

The maximum linear velocity and yaw rates are 13 m/s and 0.39 rad/s separately, which are the specifications of a hull craft type ship (shown in Figure 4) in the fleet class.³⁹ The control parameters of the proposed controllers are listed in Table 1. The simulation time step is set as 0.001 s. The initial condition for the actual USV is set as $[x(0), y(0), \theta(0), v(0), \omega(0)]^T = [15\text{m}, 15\text{m}, 0.7\text{rad}, 0\text{m/s}, 0\text{rad/s}]$. Ocean currents used in this paper are set as time-varying vector. For mathematical convenience, the vector is separated into two perpendicular directions. One component (V_x) is in the direction of x-axis in the inertial frame and another one (V_y) is in the direction of the y-axis in the inertial frame. In order to represent the variation of the ocean currents, the magnitude changes as a sine wave, $V = V_{max} \sin(at)$, which is the same form used in most studies.^{7,9} The integrated absolute error (IAE) and the time integrated absolute error (ITAE) for each test are calculated to quantitatively evaluate the transient and steady state performance of the system. The mathematical expression for the IAE and ITAE are as follow. The value of IAE and ITAE for each simulation is presented in Tables 2 and 3.

$$\begin{cases} IAE(i) = \int_0^t |i| d\tau, i = x_e, y_e \\ ITAE(i) = \int_0^t t|i| d\tau, i = x_e, y_e \end{cases} \quad (41)$$

Table 2. Performance indices of three different controllers for tracking the circular trajectory.

Control law	Circular trajectory tracking				
	IAE(x_e)	IAE(y_e)	ITAE(x_e)	ITAE(y_e)	Computational Time(s)
Backstepping	137.7	118.3	1034.3	597.9	0.7031
Normalisation	581.6	286.0	9510.0	2774.8	0.6094
PID	285.9	225.5	2908.6	2440.7	0.7969

Table 3. Performance indices of three different controllers for tracking three different scenarios.

Scenarios	BS controller				NL controller			
	IAE(x_e)	IAE(y_e)	ITAE(x_e)	ITAE(y_e)	IAE(x_e)	IAE(y_e)	ITAE(x_e)	ITAE(y_e)
2	80.1	38.9	302.1	223.5	210.4	105.3	1537.8	1891.4
3	130.2	104.6	1251.4	857.6	460.1	932.5	10792.0	27744.0
4	232.3	82.2	3310.9	820.4	211.0	205.2	1799.9	5300.0

**Figure 4.** A hull craft type ship in the fleet class.⁴⁰

Circular trajectory with constant ocean currents tracking simulation

The desired trajectory for circular trajectory tracking simulation is given as $[x_r, y_r] = [100 \cos(0.1t) - 100, 100 \sin(0.1t)]$. The constant ocean currents are set as $V_x = 1.1028\text{m/s}$ and $V_y = 0.8854\text{m/s}$.³¹ The results for the position, tracking errors and linear and angular velocity are shown in Figure 5(a) to (c). The performance indices for the three different controllers are presented in Table 2. Figure 5(a) shows that the proposed controllers are able to drive the USV to track the trajectory precisely. In contrast, PID control results in a small deviation from the desired trajectory under steady-state, as it cannot handle the ocean currents.

The detailed distinction of the steady-state and transient performance is more clearly shown in Figure 5(b) and Table 2. As it is shown in Figure 5(b), the PID controller cannot eliminate the steady-state error, which leads to poor trajectory tracking precision. In contrast, there is no steady-state error for the proposed controller. Moreover, compared with the PID controller, the BS control systems have smaller transient tracking errors, settling time, IAE and ITAE. Therefore, BS

control drives the USV to track the circular trajectory more quickly and precisely and has a superior steady state and transient performance. It is also demonstrated that the BS controller can handle the ocean currents, while the PID controller fails to tackle it. Figure 5(c) shows that the input of all the controllers is within the saturation limit. The two proposed controllers produce smoother and smaller inputs than the PID controller. With respect to the computational cost, although the PID controller requires a shorter running time than the proposed controller, the time difference between them is not obvious. Furthermore, between the two proposed controllers, the BS controller is more aggressive than the NL controller, resulting in sharper changes, especially when the tracking error is large. BS has better transient and steady state performance with less smooth inputs than the NL controller.

To sum up, compared with the PID controller, the proposed controllers have higher trajectory accuracy, better transient and steady state performance, less power consumption and close computational cost. For the proposed BS and NL controllers, the computation time for each time step (0.001 s) are only $1.6 \times 10^{-5}\text{s}$ and $1.2 \times 10^{-5}\text{s}$, respectively. Thus, a real-time solution is feasible, and thereby these controllers can be used in practical implementations.

Sinusoidal trajectory tracking with constant ocean currents simulation

A reference trajectory with varying linear and angular velocity are tracked in this simulation. The desired trajectory for the sinusoidal trajectory tracking is given as $[x_r, y_r] = [6t, 50 \sin(\frac{3\pi}{100}t)]$. The ocean currents are set as the same as in the last scenario. The simulation results are shown in Figure 6(a) to (c) and Table 3. The two controllers have a similar performance as in the case of the tracking of the circular trajectory. Both controllers

are able to converge to the desired trajectory and bound the input within the physical limits. The BS controller achieves convergence with better performance and higher precision. However, it results in a high-frequency, high-magnitude overshoot of the angular

velocity for large tracking errors, which is undesirable. The second controller has slower convergence speed but produces smoother inputs, which are also bounded within the practical limits.

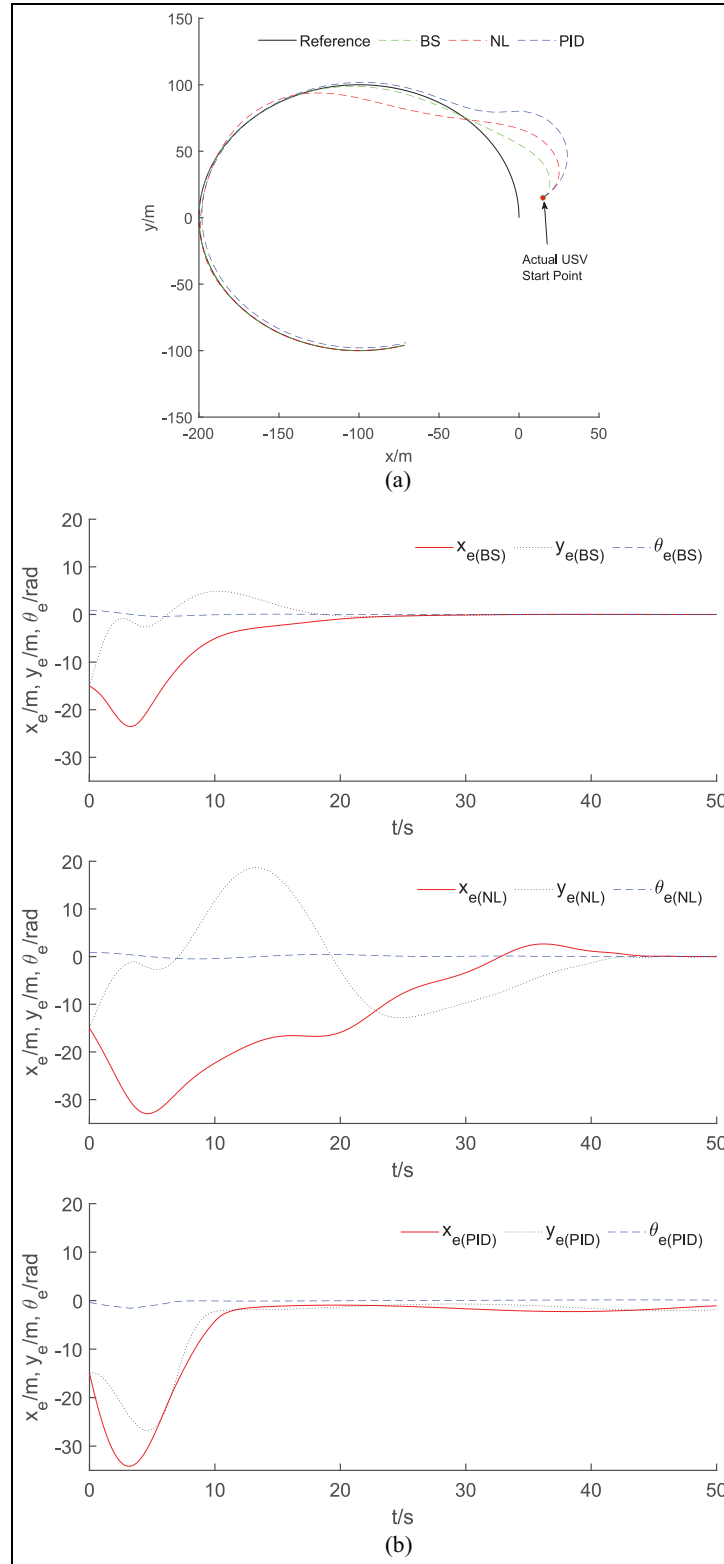


Figure 5. Continued

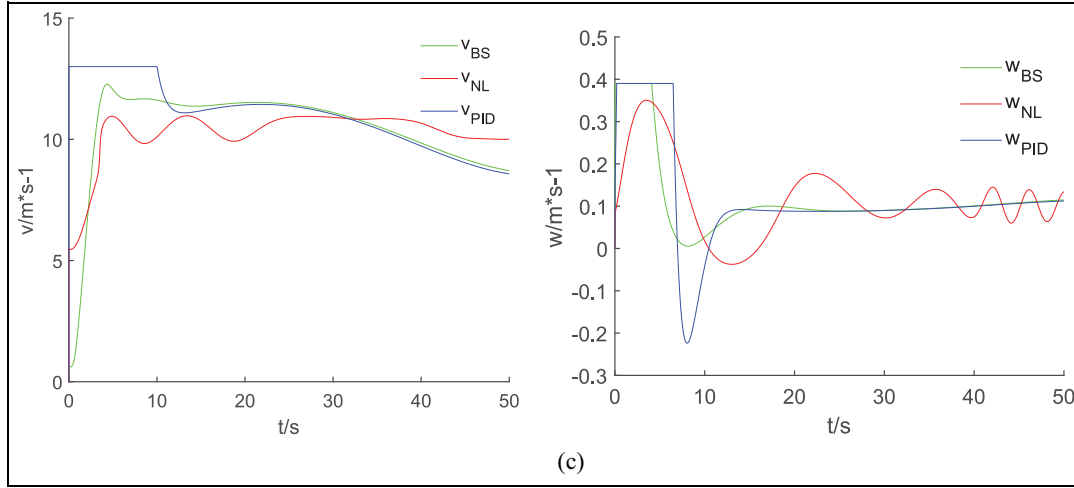


Figure 5. Result for the circular trajectory: (a) circular trajectory tracking, (b) tracking errors for the circular trajectory and (c) linear and angular velocity for the circular trajectory.

Sinusoidal trajectory tracking with time-varying ocean currents simulation

In this scenario, a more complicated sinusoidal trajectory with sharper change and time-varying ocean currents are tested. The reference trajectory is given as $[x_r, y_r] = [3t, 100 \sin(\frac{3\pi}{100}t)]$ and the time-varying ocean current are set as $V_x = 1.1028 \sin(0.2t)$ and $V_y = 0.8854 \sin(0.2t)$ m/s. The simulation results are presented in Figure 7(a) to (c) and Table 3. The figures illustrate that, in the presence of the time-varying ocean current, the BS controller takes more time but is still able to drive the system to converge to the desired trajectory. Therefore, it is still able to force the USV to track the desired trajectory and handle the input saturation with better steady-state and transient performance. For the NL controller, as the reference velocity changes more sharply, the system has damping oscillations under steady-state. Besides, the NL controller produces input that is inside the saturation limits and the yaw rate is smoother than the one for the BS controller, especially during large tracking error.

Minimum snap trajectory with time-varying ocean currents simulation

Here, a complex minimum-snap trajectory requiring the USV to smoothly pass through four stations and stop at a final station is presented. The position of the starting point and the five stations are set randomly as $[(0, 0), (60, 20), (100, -20), (240, 40), (320, 20), (400, 30)]$. The generated trajectory comprises piecewise continuous polynomials joined at each waypoint. The polynomial of each segment has the following form:

$$\begin{cases} p_{xi}(t) = p_{x0i} + p_{x1i}t + p_{x2i}t^2 + p_{x3i}t^3 + p_{x4i}t^4 + p_{x5i}t^5 \\ p_{yi}(t) = p_{y0i} + p_{y1i}t + p_{y2i}t^2 + p_{y3i}t^3 + p_{y4i}t^4 + p_{y5i}t^5 \end{cases}, t_{i-1} < t < t_i \quad (42)$$

where p_{xi} and p_{yi} are polynomial of segment i between t_{i-1} and t_i along x and y axis, respectively. $p_{x0i} \dots p_{x5i}, p_{y0i} \dots p_{y5i}$ are the corresponding coefficient. The coefficients are found so as to minimise the snap, jerk and acceleration of the USV.

The corresponding coefficient and time for each segment are shown in Table 4. The results from the test are shown in Figure 8 and Table 3. These figures show that convergence of the tracking errors can be guaranteed for the complicated minimum snap trajectory by both two controllers. However, the USV controlled by the NL controller missed the first station, thus failing to meet all the target. The BS controllers converge more quickly and can tackle the ocean currents, while the NL controller produces smoother inputs. Both controller algorithms are efficient in a realistic and challenging case study.

In conclusion, both two proposed controllers can converge the USV to the desired reference trajectory with the velocity limited inside the input saturation. The BS controller has superiority in convergence speed, steady-state performance and transient performance. Moreover, it can cancel the time-varying environmental disturbances. The NL controller produces smoother input, requires smaller computational cost but is incapable of handling the environmental disturbances. The detailed comparison between the two controllers is listed in Table 5.

Conclusion and future works

This study investigates the control methods for trajectory tracking control with motion constraints and

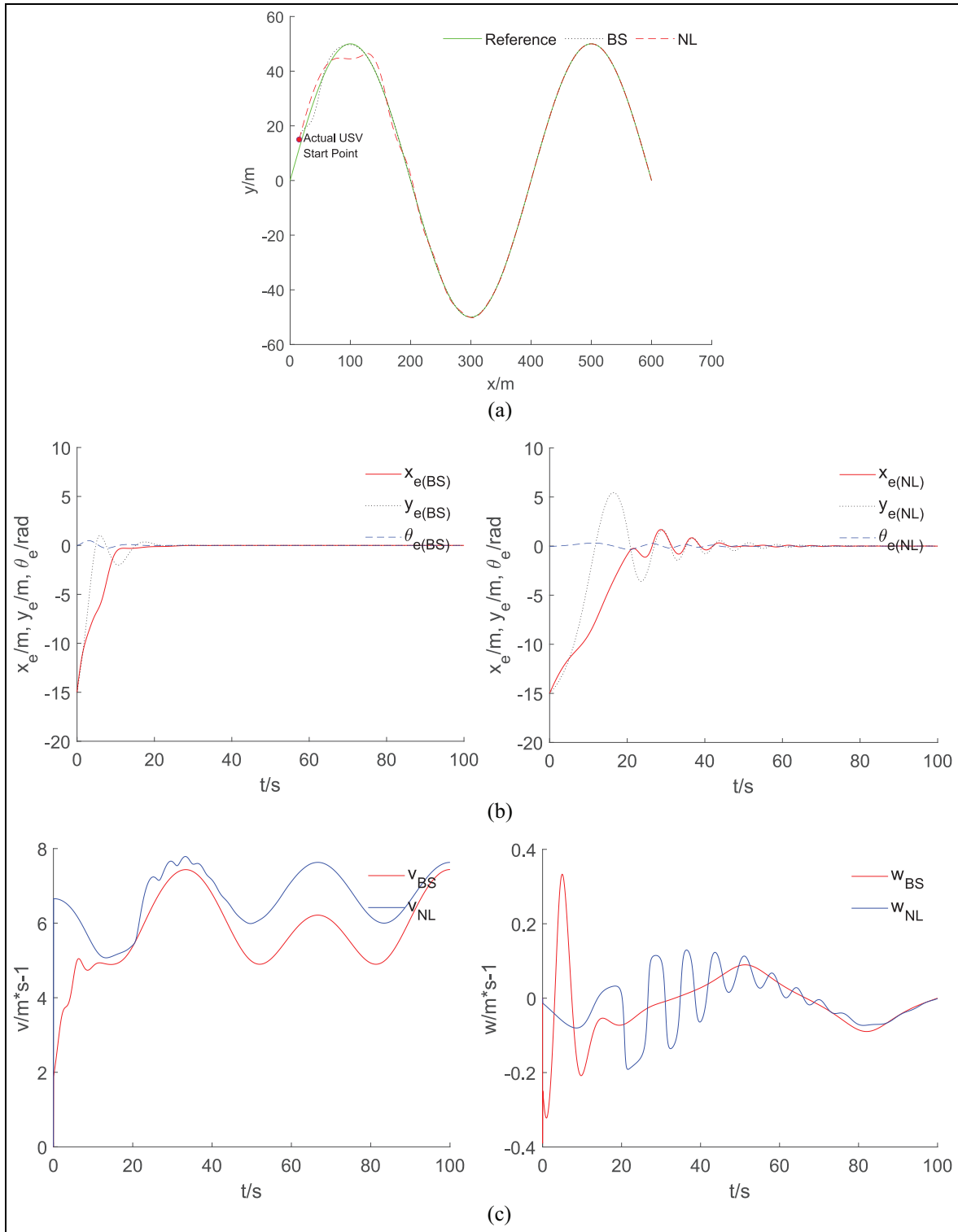


Figure 6. Simulation results for the sinusoidal trajectory: (a) sinusoidal trajectory tracking, (b) tracking errors for the sinusoidal trajectory and (c) linear and angular velocity for the sinusoidal trajectory.

environmental disturbances. For handling the disturbance, a virtual system is proposed to simplify the USV model and compensate for the environmental disturbance. Then, based on the virtual system, the backstepping technique and Lyapunov direct method are used to calculate the control law and the motion constraints

is handled by an auxiliary system. The proposed controller has a limited ability to handle input saturation. Thus, a new controller based on normalisation is designed. The tracking error is normalised in this controller and the velocity will be related to the reference and design parameters only, so that the controller can

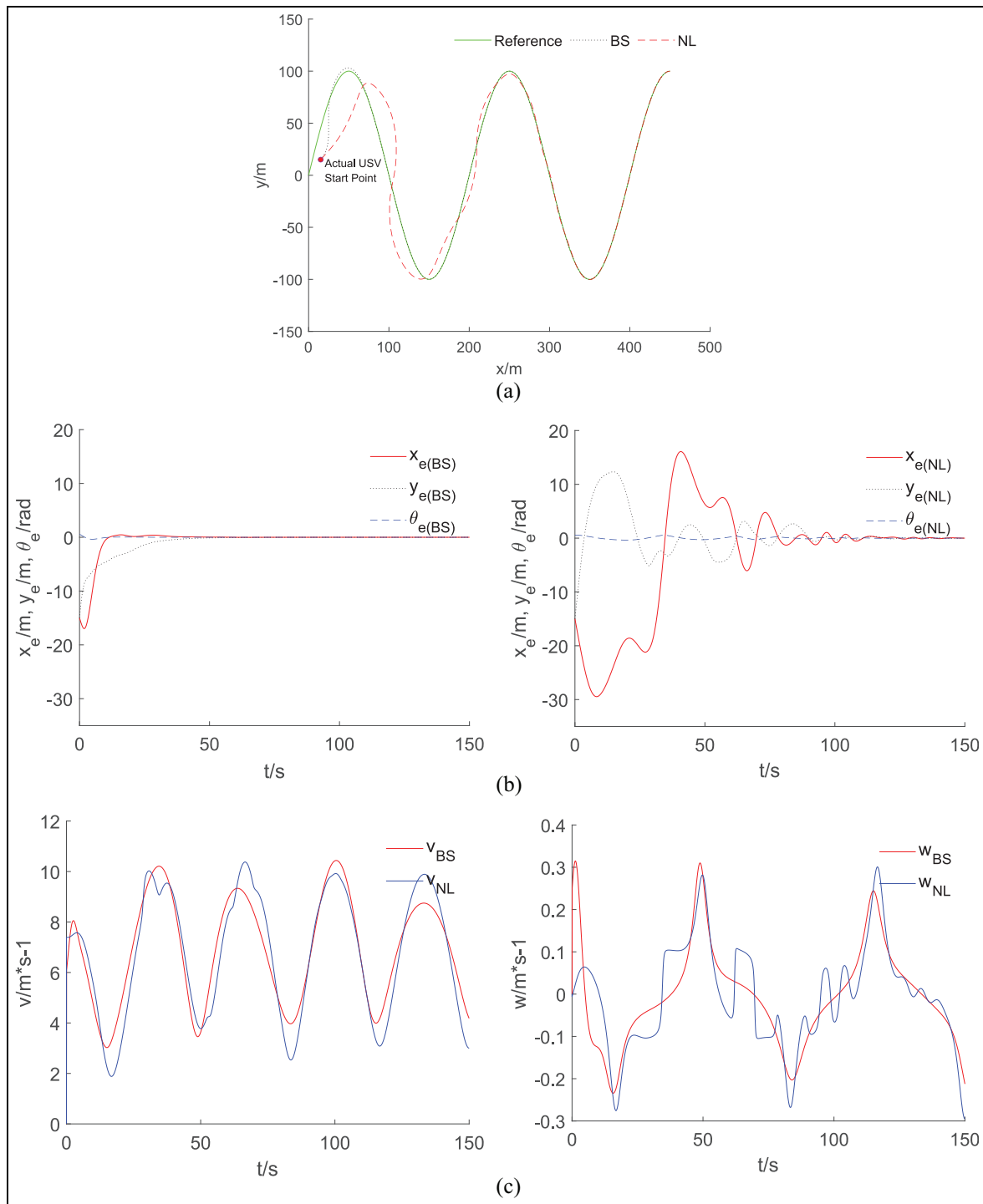


Figure 7. Sinusoidal trajectory with time-varying ocean currents: (a) sinusoidal trajectory with the time-varying ocean current, (b) tracking errors for sinusoidal trajectory with time-varying ocean currents and (c) linear and angular velocity for sinusoidal trajectory with time-varying ocean currents.

produce smoother velocity inside the motion constraints. Both controllers are able to force the USV to track the desired trajectory and handle the input saturation. Additionally, it is proved that through the use of a virtual system, even under harsh environmental disturbances like time-varying ocean currents, the system is still able to track a complicated trajectory. Moreover, the proposed controller performs better

than the common adaptive controller when the ocean currents are measurable. The two proposed methods can guarantee the uniform stability of the closed-loop system. Simulation results verify the effectiveness of the two controllers in commanding a USV for a range of trajectories and ocean current conditions. Therefore, the introduced solutions enable USVs to follow complex trajectories in a harsh marine environment.

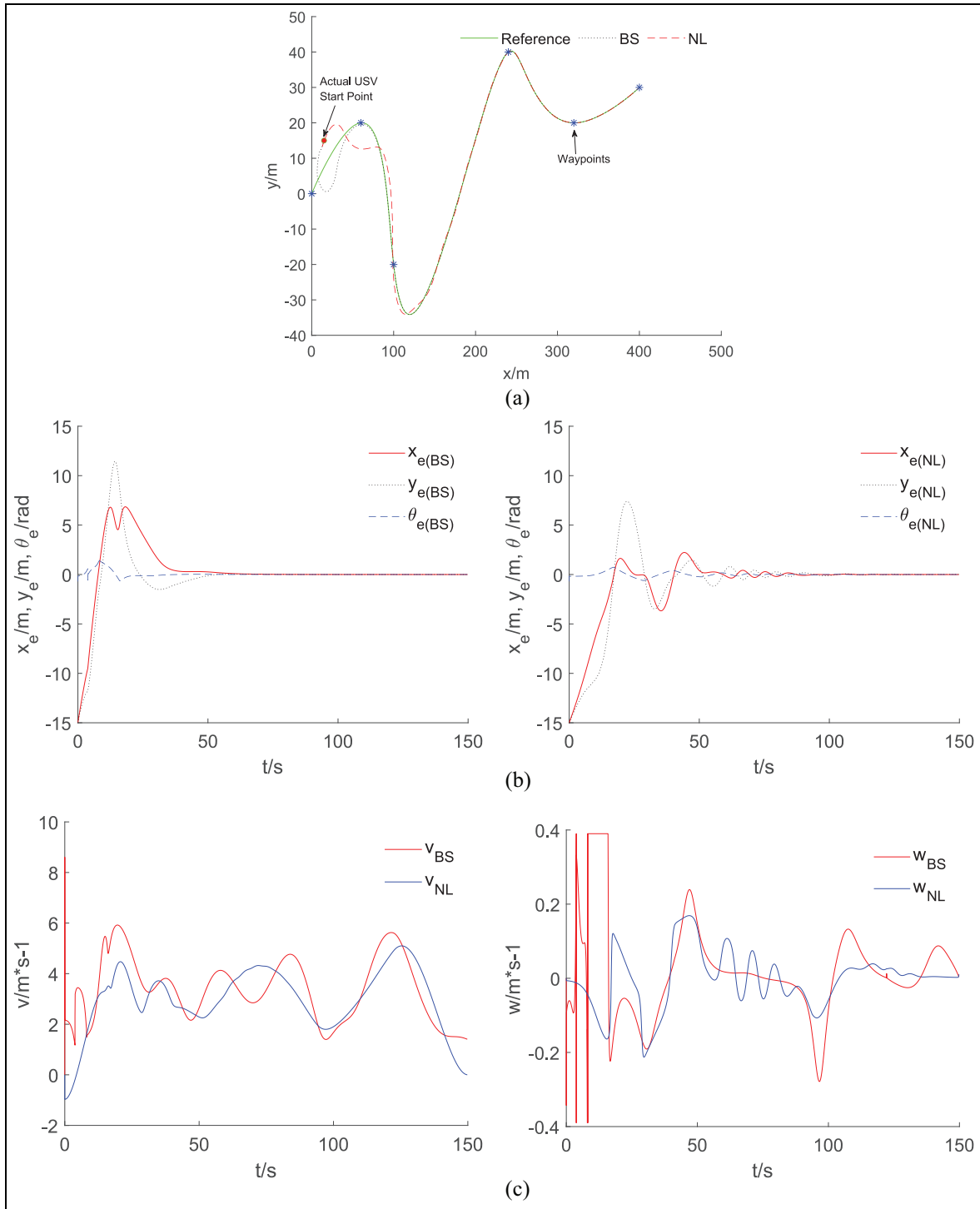


Figure 8. Minimum snap trajectory with time-varying ocean currents: (a) minimum snap trajectory with the time-varying ocean current, (b) tracking errors for sinusoidal trajectory with time-varying ocean currents and (c) linear and angular velocity for sinusoidal trajectory with time-varying ocean currents.

Future work will include incorporating the dynamic model in the design of the controller, with the dynamic uncertainties taken into consideration, as well as increasing the speed of the stabilisation action and smoothness of the inputs of the controllers. Experiments of the USV controlled by the proposed control scheme in a complex environment will also be

conducted to validate the effectiveness of the algorithms and study the real-time performance. Besides, the state constraints may also be taken into consideration and solved potentially by the Barrier Lyapunov function (BLF).

Another important research direction is to investigate the control of USVs compliant with COLREGS,

Table 4. Coefficient and time for each segment of the minimum snap trajectory.

Axis	Segment	Coefficient						Time	
		p_1	p_2	p_3	$p_4(\cdot 10^{-2})$	$p_5(\cdot 10^{-4})$	$p_6(\cdot 10^{-6})$	$t_{i-1}(s)$	$t_i(s)$
x	1	0	0	0	1.08	-3.55	3.27	0	29.08
x	2	40.71	-9.34	0.78	-1.95	2.15	-0.85	29.08	59.21
x	3	-4.05	13.58	-0.53	0.96	-0.75	0.22	59.21	92.48
x	4	-2.10	-60.51	2.41	-3.40	2.08	-0.47	92.48	121.57
x	5	12.73	357.75	-10.70	11.97	-5.90	1.08	121.57	150
y	1	0	0	0	0.52	-2.17	2.29	0	29.08
y	2	33.45	-7.70	0.64	-1.99	2.52	-1.12	29.08	59.21
y	3	-4.75	21.52	-1.09	1.96	-1.48	0.40	59.21	92.48
y	4	-1.73	-52.66	1.83	-2.30	1.25	-0.25	92.48	121.57
y	5	4.81	137.71	-3.97	4.28	-2.04	0.36	121.57	150

Table 5. Comparison between the BS and NL controller.

Controller	BS	NL
Method	Backstepping technique	Normalisation technique
Pros	Environmental disturbance cancellation Larger convergence speed Better steady state/transient performance Limiting the velocity inside the input saturation	Smoother control input Smaller computational cost Lower power consumption rate Limiting the velocity inside the input saturation
Cons	Sharp velocity change (especially at velocity limit) Long-period maximum load	Ignorance of environmental disturbances Poor performance for sharp reference velocity change
Applicable Environment	Environment with large disturbance: For example, ocean with harsh weather Complex trajectory with sharp velocity change: For example, reefs High/medium-speed USVs ($\geq 10knots$): For example, Tianxing No. 1 ⁴³	Environment with small disturbance: For example, broad and smooth lake/river Low-speed USVs ($\leq 10knots$): For example, Springer ⁴¹ and Charlie ⁴² Large USVs with high power: For example, Fleet Class USVs ⁴⁰

which is an international traffic regulation for preventing collisions at sea. A plausible strategy to achieve this is to integrate sensing and planning modules with the controllers. For example, an appropriate moving obstacle detection system (based upon radar, AIS or visual systems) should be first investigated to capture the navigational information of moving ships in real-time. Then, the collision risks should be properly assessed by using DCPA/TCPA⁴⁴ or ship domains,⁴⁵ which will facilitate path planning algorithms to generate COLREGs compliant collision free trajectories and enable path following controllers to track.

It also should be noted that before real implementation, the proposed trajectory tracking control solution will need to be complemented with collision avoidance approaches. In particular, the extension to multi-agent systems will require the consideration of both internal and external obstacles, with many alternative methods being applicable for formation control and cooperative motion planning. Specific strategy could be that the artificial potential field method⁴⁶ can be first implemented to model and evaluate the collision risks imposed by obstacles. Path planning algorithms such as the constrained A* algorithm⁴⁷ will then be employed to generate collision free trajectories, which will finally robustly be tracked using the controller developed in this paper.



Declaration of conflicting interests

The author(s) declared no potential conflicts of interest with respect to the research, authorship, and/or publication of this article.

Funding

The author(s) disclosed receipt of the following financial support for the research, authorship, and/or publication of this article: This work is partially supported by Royal Society (Grant no. IEC\NSFC\191633).

ORCID iDs

Yuanchang Liu  <https://orcid.org/0000-0001-9306-297X>
 Enrico Anderlini  <https://orcid.org/0000-0002-8860-8330>

References

1. Tanakitkorn K. A review of unmanned surface vehicle development. *Mar Technol Res* 2019; 1: 2–8.
2. Azzeri MN, Adnan FA and Zain MZ. Review of course keeping control system for unmanned surface vehicle. *J Teknol* 2015; 74: 11–20.
3. Liu Z, Zhang Y, Yu X, et al. Unmanned surface vehicles: an overview of developments and challenges. *Annu Rev Control* 2016; 41: 71–93.

4. NađĐ, Mišković N and Mandić F. Navigation, guidance and control of an overactuated marine surface vehicle. *Annu Rev Control* 2015; 40: 172–181.
5. Shi Y, Shen C, Fang H, et al. Advanced control in marine mechatronic systems: a survey. *IEEE ASME Trans Mechatron* 2017; 22: 1121–1131.
6. Ashrafioun H, Muske KR and McNinch LC. Review of nonlinear tracking and setpoint control approaches for autonomous underactuated marine vehicles. In: *Proceedings of the 2010 American control conference*, Baltimore, MD, 30 June–2 July 2010, pp.5203–5211. New York: IEEE.
7. Fan Y, Huang H and Tan Y. Robust adaptive path following control of an unmanned surface vessel subject to input saturation and uncertainties. *Appl Sci* 2019; 9(9): 1815.
8. Liu T, Dong Z, Du H, et al. Path following control of the underactuated USV based On the improved line-of-sight guidance algorithm. *Pol Marit Res* 2017; 24: 3–11.
9. Zheng Z and Sun L. Path following control for marine surface vessel with uncertainties and input saturation. *Neurocomputing* 2016; 177: 158–167.
10. Fossen TI. *Handbook of marine craft hydrodynamics and motion control*. UK: John Wiley & Sons, 2011.
11. Fuguang D, Yuanhui W and Yong W. Trajectory-tracking controller design of underactuated surface vessels. In: *OCEANS'11 MTS/IEEE KONA*, Waikoloa, HI, 19–22 September 2011, pp.1–5. New York: IEEE.
12. Huang J, Wen C, Wang W, et al. Global stable tracking control of underactuated ships with input saturation. *Syst Control Lett* 2015; 85: 1–7.
13. Zheng H, Negenborn RR and Lodewijks G. Trajectory tracking of autonomous vessels using model predictive control. *IFAC Proc Vol* 2014; 47: 8812–8818.
14. Chwa D. Global tracking control of underactuated ships with input and velocity constraints using dynamic surface control method. *IEEE Trans Control Syst Technol* 2011; 19: 1357–1370.
15. Serrano ME, Scaglia GJE, Godoy SA, et al. Trajectory tracking of underactuated surface vessels: a linear algebra approach. *IEEE Trans Control Syst Technol* 2014; 22: 1103–1111.
16. Larrazabal JM and Peñas MS. Intelligent rudder control of an unmanned surface vessel. *Expert Syst Appl* 2016; 55: 106–117.
17. Pettersen KY and Egeland O. Exponential stabilization of an underactuated surface vessel. In: *Proceedings of 35th IEEE conference on decision and control*, Kobe, Japan, 13 December 1996, vol. 961, pp.967–972. New York: IEEE.
18. Dong Z, Wan L, Li Y, et al. Trajectory tracking control of underactuated USV based on modified backstepping approach. *Int J Nav Archit Ocean Eng* 2015; 7: 817–832.
19. Wang H and Zhang S. Event-triggered reset trajectory tracking control for unmanned surface vessel system. *Proc IMechE, Part I: J Systems and Control Engineering* 2021; 235: 633–645.
20. Chen WH. Disturbance observer based control for nonlinear systems. *IEEE ASME Trans Mechatron* 2004; 9: 706–710.
21. Fossen TI and Lekkas AM. Direct and indirect adaptive integral line-of-sight path-following controllers for marine craft exposed to ocean currents. *Int J Adapt Control Signal Process* 2017; 31(4): 445–463.
22. Zhu G and Du J. Global robust adaptive trajectory tracking control for surface ships under input saturation. *IEEE J Oceanic Eng* 2020; 45: 442–450.
23. Qiu B, Wang G, Fan Y, et al. Adaptive sliding mode trajectory tracking control for unmanned surface vehicle with modeling uncertainties and input saturation. *Appl Sci* 2019; 9: 1240.
24. Flagg CN, Schwartz G, Gottlieb E, et al. Operating an acoustic doppler current profiler aboard a container vessel. *J Atmos Ocean Technol* 1998; 15: 257–271.
25. Mostafa MZ, Khater HA, Rizk MR, et al. GPS/DVL/MEMS-INS smartphone sensors integrated method to enhance USV navigation system based on adaptive DSFCF. *IET Radar Sonar Navig* 2019; 13: 1616–1627.
26. Ziyue Z, Haiou L, Huiyan C, et al. Tracking control of unmanned tracked vehicle in off-road conditions with large curvature *. In: *2019 IEEE intelligent transportation systems conference (ITSC)*, Auckland, New Zealand, 27–30 October 2019, pp.3867–3873. New York: IEEE.
27. Chen C, Li J, Li M, et al. Model predictive trajectory tracking control of automated guided vehicle in complex environments. In: *2018 IEEE 14th international conference on control and automation (ICCA)*, Anchorage, AK, 12–15 June 2018, pp.405–410. New York: IEEE.
28. Wang D, Wei W, Yeboah Y, et al. A robust model predictive control strategy for trajectory tracking of omni-directional mobile robots. *J Intell Robot Syst* 2020; 98: 439–453.
29. Yan X, Jiang D, Miao R, et al. Formation control and obstacle avoidance algorithm of a multi-USV system based on virtual structure and artificial potential field. *J Mar Sci Eng* 2021; 9: 161.
30. Yang Q, Fang H, Cao M, et al. Distributed trajectory tracking control for multiple nonholonomic mobile robots**This work was supported by Projects of Major International (Regional) Joint Research Program (No.61120106010), National Science Foundation for Distinguished Young Scholars of China (No.60925011), National Natural Science Foundation of China (No.61175112), Program for New Century Excellent Talents in University, and the Specialized Research Fund for the Doctoral Program of Higher Education of China (20111101110011). *IFAC PapersOnLine* 2016; 49: 31–36.
31. Belleter DJW and Pettersen KY. Path following for formations of underactuated marine vessels under influence of constant ocean currents. In: *53rd IEEE conference on decision and control*, Los Angeles, CA, 15–17 December 2014, pp.4521–4528. New York: IEEE.
32. Abdelaal M, Fränzle M and Hahn A. Nonlinear model predictive control for trajectory tracking and collision avoidance of underactuated vessels with disturbances. *Ocean Eng* 2018; 160: 168–180.
33. Li H, Yan W and Shi Y. Continuous-time model predictive control of under-actuated spacecraft with bounded control torques. *Automatica* 2017; 75: 144–153.
34. Liang H, Li H and Xu D. Nonlinear model predictive trajectory tracking control of underactuated marine vehicles: theory and experiment. *IEEE Trans Ind Electron* 2021; 68: 4238–4248.
35. Li H and Yan W. Model predictive stabilization of constrained underactuated autonomous underwater vehicles

- with guaranteed feasibility and stability. *IEEE ASME Trans Mechatron* 2017; 22: 1185–1194.
36. Mellinger D and Kumar V. Minimum snap trajectory generation and control for quadrotors. In: *2011 IEEE international conference on robotics and automation*, Shanghai, Chin, 9–13 May 2011, pp.2520–2525. New York: IEEE.
 37. Ren P, Zhao N and Wang Y. Trajectory tracking of wheeled robot based on feedforward compensation PID. *J Henan Univ Eng* 2020; 32(11): 60–62 + 71.
 38. Bertrand S, Guénard N, Hamel T, et al. A hierarchical controller for miniature VTOL UAVs: design and stability analysis using singular perturbation theory. *Control Eng Pract* 2011; 19: 1099–1108.
 39. Kim H, Kim D, Shin J-U, et al. Angular rate-constrained path planning algorithm for unmanned surface vehicles. *Ocean Eng* 2014; 84: 37–44.
 40. Navy US. The Navy unmanned surface vehicle (USV) master plan, https://www.rand.org/content/dam/rand/pubs/research_reports/RR300/RR384/RAND_RR384.pdf (2007, accessed 18 October 2020).
 41. Sutton R, Sharma S and Xiao T. Adaptive navigation systems for an unmanned surface vehicle. *J Mar Eng Technol* 2011; 10: 3–20.
 42. Caccia M, Bibuli M, Bruzzone G, et al. Charlie, a testbed for USV research. *IFAC Proc Vol* 2009; 42: 97–102.
 43. Zhuang J, Zhang L, Wang B, et al. Navigating high-speed unmanned surface vehicles: system approach and validations. *J Field Robot* 2021; 38: 619–652.
 44. Chen X, Liu Y, Achuthan K, et al. A ship movement classification based on automatic identification system (AIS) data using convolutional neural network. *Ocean Eng* 2020; 218: 108182.
 45. Szlapczynski R, Krata P and Szlapczynska J. Ship domain applied to determining distances for collision avoidance manoeuvres in give-way situations. *Ocean Eng* 2018; 165: 43–54.
 46. Mina T, Singh Y and Min B-C. Maneuvering ability-based weighted potential field framework for multi-USV navigation, guidance, and control. *Mar Technol Soc J* 2020; 54: 40–58.
 47. Singh Y, Bibuli M, Zereik E, et al. A novel double layered hybrid multi-robot framework for guidance and navigation of unmanned surface vehicles in a practical maritime environment. *J Mar Sci Eng* 2020; 8: 624.
 48. Wen L, Yan J, Yang X, et al. Collision-free trajectory planning for autonomous surface vehicle. In: *2020 IEEE/ASME international conference on advanced intelligent mechatronics (AIM)*, Boston, MA, 6–9 July 2020, pp.1098–1105. New York: IEEE.